SENSITIVITY, RESOLUTION AND AMBIGUITY OF THE CRS STACK OPERATOR

L.W.B. Leite and W.W.S. Vieira

email: *lwbleite@gmail.com*
keywords: *CRS stack, ambiguity, resolution, sensitivity*

ABSTRACT

This report describes an investigation about the sensitivity and ambiguity of the CRS stack operator with respect to 4 parameters ($v_0, R_{NIP}, R_N, \alpha_0$), and its resolution in terms of the statistical properties of the solution of a nonlinear multi-parametric optimization problem for curve fitting in the least-square sense. The sensitivity method is borrowed from dynamic system analysis and synthesis, and the definitions are based on the Miller-Murray model. One of the main major aim is to compare the results on the sensitivity parameters to the strategy for the CRS attributes search.

As a result of a parallel investigation of optimization techniques is the combination of global and local methods to reach the minimum, around which linearity is a better relation between the linear and the non-linear counterpart of the optimization problem and its solution. A first search should look a minimum with a method of controlled random type, followed by a second search to perform a last iteration using a gradient method to obtain the data and parameter resolution and covariance matrices, and further statistical properties.

The sensitivity functions are represented by the columns of the problem matrix, and they exhibit a linear behavior of the operator instead of a concave form, and this linearity informs the necessity of a good starting point for the search of the parameters.

INTRODUCTION

The motivations of the present work start from two aspects of the CRS (Common Reflection Surface) stack: (1) the presence of noise in the recovered attributes; and (2) the strategy of the parameter search. The analysis of the CRS stack results (sections: stack, coherence, migration, R_{NIP}, R_N, α_0) show that as the observed input data improves on the signal/noise ratio, the attribute sections show a structure that resembles more the stack section that is used as reference. Sensitivity analysis can be used to determine how sensitive the model is to changes in the value of the parameters of the model, and to changes in the structure of the model.

This report is structured in three main parts related to curve fitting, between synthetic data and the forward model represented by the CRS stack operator, as an optimization problem in the least-square sense. The parts are: (1) Controlled random global search for the parameters; (2) second order gradient method, resolution and ambiguity; and (3) sensitivity analysis and its relation to the CRS attributes search.

Sensitivity and ambiguity calculus is to be performed directly in the forward model as a first step in the analysis of the data fitting problem, and it is independent of the object function and of the mathematical problem defined as optimization. This calculus is used for the purpose of analysis and synthesis of mathematical models. In order to be able to give a unique formulation of the mathematical problem, the mathematical model is usually considered to be known exactly, but this assumption is unrealistic since there is always a certain discrepancy between the actual system (data) and its mathematical model (operator). This discrepancy results from the following partial reasons:

- A real system cannot be identified exactly because of the restricted accuracy of the measuring devices;

- Mathematical models are often simplified or idealized intentionally in order to simplify the mathematical problem or to make it solvable at all.

For these reasons, the results of mathematical synthesis need not necessarily be practicable, or they may even be very poor, if there is considerable deviations between the real system and the mathematical model, and the solution be very sensitivity to the parameters. Therefore, it should be part of the practical problem to learn about parameter sensitivity prior to its implementation, or to reduce the sensitivity systematically if this turns out to be necessary.

This is important if one is involved in optimization procedures, since a natural property of optimization is to extremize the performance of a certain set of parameters that controls the operation. Example of this are gradient methods, adaptive and self-learning systems.

Among the major aims the present study are: (1) to analyze the sensitivity of the CRS hyperbolic stack operator to its parameters; and (2) to compare the results of the analysis of the parameter sensitivities with the strategy for the CRS attribute search as described by Muller (1999) and Mann (2002).

The parameter search here discussed is organized as a nonlinear optimization problem, and statistical properties in the optimization process shows up when derivative methods are applied, in particular when the norm-2 is applied due to simplicity and elegance, as described by Tarantola (1984). Data and parameter resolution matrices and unit covariance matrix are calculated and analyzed on the basis of the linearized nonlinear problem based on Taylor series expansion to the first order.

The CRS parameter search strategies in the semblance domain is divided in two main parts: (1) the first part is a search to determine initial parameter values to start the optimization iterations; (2) a second part is a simultaneous search for all parameters starting from the initial values. The searches are performed in the CMP (Common Mid Point) families of the data cube.

The forward model is represented by the CRS stack operator in terms of $t(x_m, h; \mathbf{m})$, and the optimization problem as a fitting between the predictive surface $t^{pre}(x_m, h; \mathbf{m})$ and the observed data $t^{obs}(x_m, h)$. The least-square fitting was chosen as the object function of optimization, and the problem is classified as nonlinear, multi-parametric, overdetermined, and to avoid local minima it is proposed a solution by the combination of Controlled Random Search Global method (CRSG), and of a gradient method (GM) that allows for the statistical analysis of the solution. The combination of these methods follows the principle that CRSG defines a region around the global minimum, theoretically well defined, followed by a last iteration around a minimum with linear properties in order to construct the correlation and resolution matrices. The numerical experiments were realized for randomly chosen points $P_0(x_0, t_0)$; so, neither to extend along the traces, $(t_0 = 0, t_{total})$, nor along the mid-points $(x_0 = 0, x_{total})$. As established, the solution by the CRSG method is used as input to the GM method, but in the present work these experiments were realized separately.

The structure of the sensitivity analysis is based on the polynomial function of the CRS operator represented by $t(x_m, h; v_0, R_{NIP}, R_N, \alpha_0)$, where the quantitative properties of this system with respect to its parameters $(v_0, R_{NIP}, R_N, \alpha_0)$, are shown as functions of the independent variables x_m e h.

The original seismic problem is presented in the following form: Given an observed seismic section $t^{obs}(x_m, h)$ in the data space D, one wishes to find a model $\mathbf{m}$ in the parameter space M such that the forward model $t^{pre}(x_m, h)$ fits the observed data in the least-square sense.

The methodology for sensitivity analysis has been borrowed from the analysis and design of dynamic systems, as described, e.g., by Frank (1978) for engineering applications, and by many others for partial differential equations, e.g., Saltelli et al. (2004). Among the several methods for uncertainty and sensitivity analysis, the method adopted here is the local method which is based on a derivative.

The basic definitions to quantify the parameter sensitivity of a system is summarized in the sequel, but we start adjusting the classical nomenclature to our model; therefore, we start defining the direct model.

DIRECT MODEL

The direct model is the CRS stack operator that describes the impulse traveltime for curved reflectors based on the paraxial ray theory, and takes into account only primary reflection trajectories (Mann (2002)). The

equation, represented physically by Figure 1, is given by:

$$t(x_m, h; \mathbf{m}) = \sqrt{\left[t_0 + \frac{2\sin\alpha_0(x_m - x_0)}{v_0}\right]^2 + \frac{2t_0\cos^2\alpha_0}{v_0}\left[\frac{(x_m - x_0)^2}{R_N} + \frac{h^2}{R_{NIP}}\right]}. \tag{1}$$

In the above equation (1), the independent variables are x_m e h, respectively, the mid-point and the half-offset in the CMP configuration, as is shown in Figure 2, and the parameters to be analyzed are $\mathbf{m} =$(v_0, R_{NIP}, R_N and α_0) related to the reference point $P_0(x_0, t_0)$. v_0 is the velocity of the upper layer and, in practical work defined as a fixed value around $P_0(x_0, t_0)$, but here taken as a parameter to be analyzed. α_0 is the vertical emergence angle of the wave front. The quantities R_{NIP} and R_N are the wave front curvature related, respectively, to the Normal Incident Wave (NIP-wave) and to the Normal wave (N-wave). To satisfy the paraxial ray theory, a central ray of reference must established, and in this case it is taken the zero offset ray between the surface observation point and the normal incidence point in subsurface. The central ray satisfies Snell's law through the interfaces, and the wave front curvatures of the NIP and N waves change according to the refraction and transmission laws.
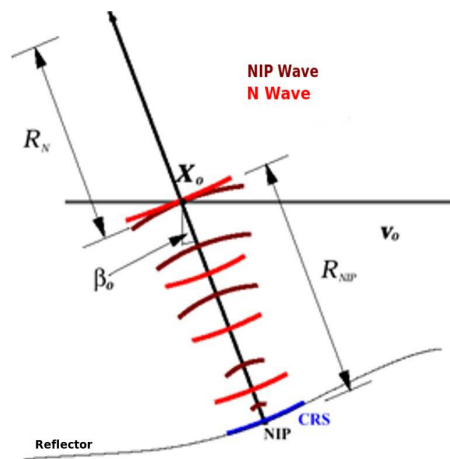
Figure 1: Physical illustration of the CRS model formed by one layer over a half-space separated by a curved interface.
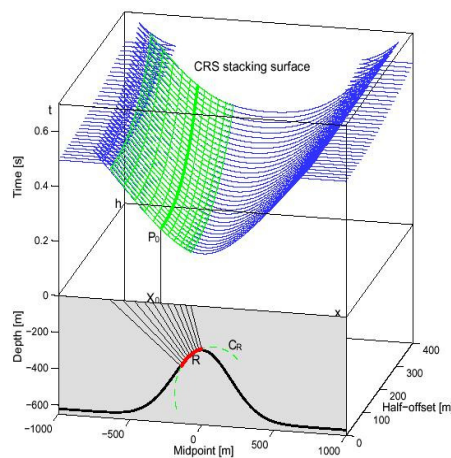
Figure 2: 3-D perspective representing the CRS operator in green [equation (1)] and the observed data in blue.

Bernabini et al. (1987) describe functionals to be evaluated quantitatively on a given CMP gather for the goodness of fit between data and a model function, particularly for a stacking velocity value of the hyperbolic reflection response. The most common functionals measure the likeness of the corrected gather's amplitude traces ($\overline{u}$) based on correlation of traces, and choices of normalization. The normalized 2D (x_m, h) measure semblance $Sen(t_0; \mathbf{m})$ is composed by averages, and it is given by:

$$Sen(t_0; \mathbf{m}) = \frac{\frac{1}{N_t}\sum_{t=t_0-\delta t}^{t=t_0+\delta t}\frac{1}{N_{x_m}}\sum_{x_m=x_F}^{x_m=x_L}\left[\frac{1}{N_h}\sum_{h=h_F}^{h=h_L}\overline{u}(x_m, h; t_0)\right]^2}{\frac{1}{N_t}\sum_{t=t_0-\delta t}^{t=t_0+\delta t}\frac{1}{N_{x_m}}\sum_{x_m=x_F}^{x_m=x_L}\frac{1}{N_h}\sum_{h=h_F}^{h=h_L}\overline{u}^2(x_m, h; t_0)}, \quad (\text{where} \quad 0 \leq Sen \leq 1); \quad (2)$$

where the set of parameters $\mathbf{m}$ are related to the trajectory of the summation defined by equation (1), from a near first $h = h_F$ to a last $h = h_L$ offset with N_h points, from a near first $x_m = x_F$ to a last $x_m = x_L$ mid-point with N_x points, and in a time window specified by some δt around t_0. $Sen(t_0; \mathbf{m})$ takes values in the interval (0,1) regardless of the signal amplitude, and it quantifies the uniformity of the signal polarity across the NMO (Normal Moveout) corrected gather amplitude $\overline{u}(t_0)$. This equation does not carry implicitly information about the model $t^{pre}(x_m, h)$; therefore, cannot be used directly as a curve fitting measure.

Figure 3 serves to represent the semblance function (2), where the aim of the optimization is to search for the global minimum represented in red. Local minima can also be seen by yellow spots. As Muller (1999) addresses to the CRS stack objective function, he shows plots of equation (2) in form of cube perspectives and slices as maps of R_{NIP} versus R_N, R_{NIP} versus α, R_{NIP} versus R_N, R_N versus α, where the global minimum present very clearly elongated forms that we call valleys. Figure 4 represents the forward model without noise, and Figure 5 represents the synthetic data. Both informations were calculated
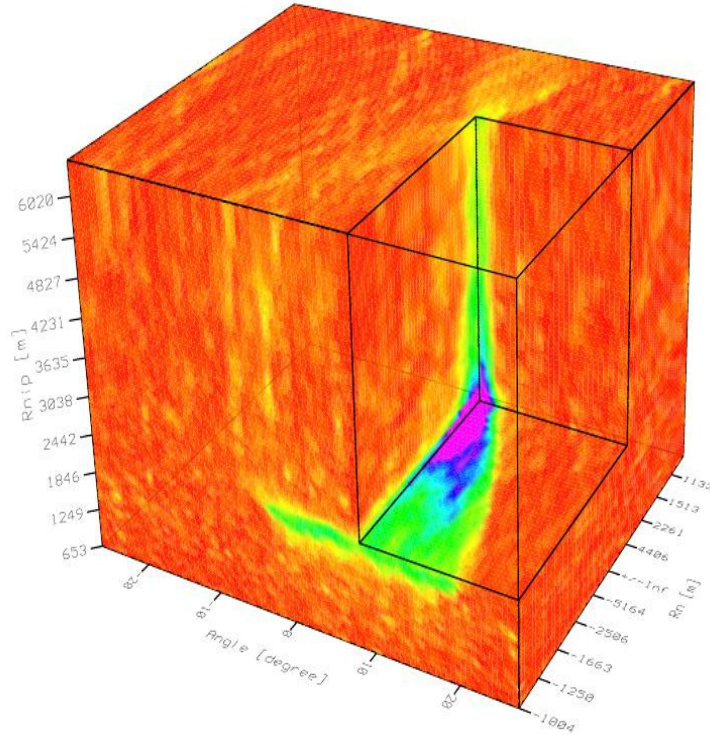
Figure 3: Perspective of the coherence values given by equation (2) as function of the wavefield attributes α_0, R_N and R_{NIP}.
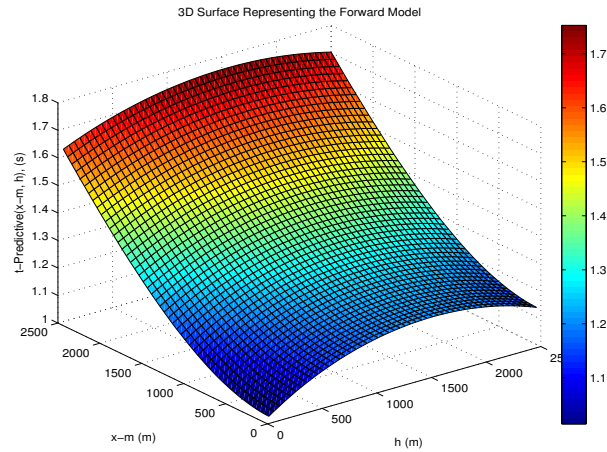
Figure 4: 3-D perspective that represents the forward model calculated by equation (1) showing the hyperbolic aspect.
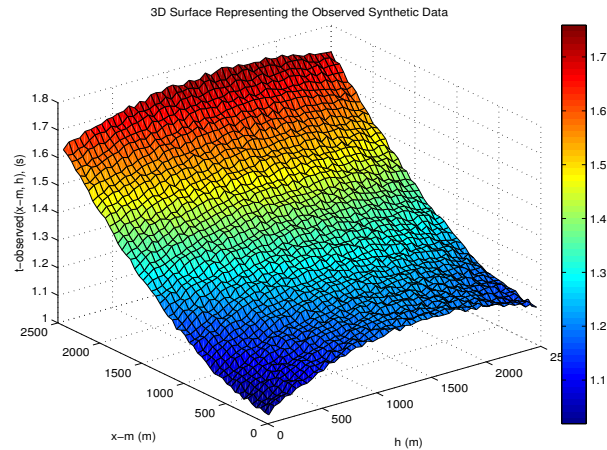
Figure 5: 3-D perspective that represents the synthetic data calculated by equation (1) with random noise added showing the hyperbolic aspect.

by equation (1), where random noise from a normal distribution has been added and controlled visually. Therefore, this study does not have picked events, inclusive in the semblance sense.

SENSITIVITY MODEL

The system function is denoted by $\mathbf{t} = \mathbf{t}(\mathbf{m})$, dependent on the parameter vector $\mathbf{m} = [m_1, m_2, \dots m_M]^T$, and in our problem we have that $\mathbf{m}$ is specifically given by $\mathbf{m} = [v_0, R_{NIP}, R_N, \alpha_0]^T$. The nominal parameters and system function are denoted with the lower script 0: $\mathbf{m}_0$ and $\mathbf{t}_0$. Considering continuity conditions, the following definitions for the sensitivity function, $\mathbf{S}$, are applied.

- Absolute sensitivity function:

$$\mathbf{S}_j \triangleq \left. \frac{\partial \mathbf{t}(\mathbf{m})}{\partial m_j} \right|_{\mathbf{m}_0} = \mathbf{S}_j(\mathbf{m}_0), \quad (j = 1, 2, \dots M). \tag{3}$$

The parameter-induced error of the system function is written by:

$$\Delta t \triangleq \sum_{j=1}^{j=M} \mathbf{S}_j \Delta m_j; \tag{4}$$

and the maximum error by

$$|\Delta t| \triangleq \sum_{j=1}^{j=M} |\mathbf{S}_j||\Delta m_j|, \tag{5}$$

where the vertical bars stand for the absolute values of the elements of the corresponding vector $\mathbf{m}$ or $\mathbf{S_j}$.

- Relative logarithmic sensitivity function:

$$\overline{\mathbf{S}}_j \triangleq \frac{\partial \ln \mathbf{t}(\mathbf{m})}{\partial \ln m_j}\bigg|_{m_0} = \overline{\mathbf{S}}_j(\mathbf{m}_0), \quad (j = 1, 2, ...M). \tag{6}$$

The $\ln \mathbf{m}$ means the vector of the logarithms of the elements of $\mathbf{m}$, therefore $\partial \ln \mathbf{m} = [\partial\, m_1/m_1\, m_2/m_2 \ldots m_M/m_M]_T t$. The ith element of $\overline{\mathbf{S}}_j$ is expressed by:

$$\overline{S}_{ij} = \frac{\partial\, t_i/t_i}{\partial\, m_j/m_j}\bigg|_{m_0} = S_{ij}\frac{m_{j0}}{t_{i0}}, \quad (i = 1, 2, ...N;\ j = 1, 2, ...M). \tag{7}$$

where S_{ij} is the ijth element of absolute sensitivity function $\mathbf{S}_j$. The ith element of the relative error of the system function is expressed as:

$$\frac{\Delta t_i}{t_{i0}} \triangleq \sum_{j=1}^{j=M} \mathbf{S}_{ij}\frac{\Delta m_j}{m_{j0}}, \quad (i = 1, 2, \ldots, N); \tag{8}$$

and the maximum relative error of the system function is given by

$$|\frac{\Delta t_i}{t_{i0}}| \triangleq \sum_{j=1}^{j=M} |\mathbf{S}_{ij}||\frac{\Delta m_j}{m_{j0}}|, \quad (i = 1, 2, \ldots, N). \tag{9}$$

There are also two ways to define a semi-relative sensitivity function as follows.

- Upper-semi-relative logarithmic sensitivity function:

$$\check{\mathbf{S}}_j \triangleq \frac{\partial \ln \mathbf{t}(\mathbf{m})}{\partial m_j}\bigg|_{\mathbf{m}_0}, \quad (j = 1, 2, ...M). \tag{10}$$

The components $\check{S}_{ij}$ are given by:

$$\check{S}_{ij} = \frac{\partial\, \mathbf{t_i}/t_i}{\partial m_j}\bigg|_{\mathbf{m}_0} = \frac{1}{t_{i0}}S_{ij}, \quad (i = 1, 2, ...N),\ (j = 1, 2, ...M). \tag{11}$$

- Lower-semi-relative logarithmic sensitivity function:

$$\hat{\mathbf{S}}_j \triangleq \frac{\partial \mathbf{t}(\mathbf{m})}{\partial \ln m_j}\bigg|_{\mathbf{m}_0}, \quad (j = 1, 2, ...M). \tag{12}$$

The components $\hat{S}_{ij}$ are given by:

$$\hat{S}_{ij} = \frac{\partial\, \mathbf{t_i}}{\partial m_j/m_j}\bigg|_{\mathbf{m}_0} = m_{0j}S_{ij}, \quad (i = 1, 2, ...N),\ (j = 1, 2, ...M). \tag{13}$$

INVERSE MODEL

The short description to follow is to present a relation between the optimization technique and the sensibility analysis for completeness. In this way, Vieira and Leite (2009) and Santos et al. (2009) presented strategies with two optimization methods combined to investigate the convergence and resolution of the CRS operator aiming at practical applications. The concepts involved: (1) Random Controlled Search (known also as Price method) and Gradient Method (known also as Gauss-Newton, or Second Order Gradient). The misfit measure used for reference, $\phi(\mathbf{m})$, is expressed as:

$$\phi(\mathbf{m}) = \sqrt{\frac{\sum_{i=1}^{N} [t_i^{obs} - t_i^{pre}(\mathbf{m})]^2}{N}}. \tag{14}$$

This measure is not to be confused with the semblance function, and Figure 6 show the layout of the inversion process.
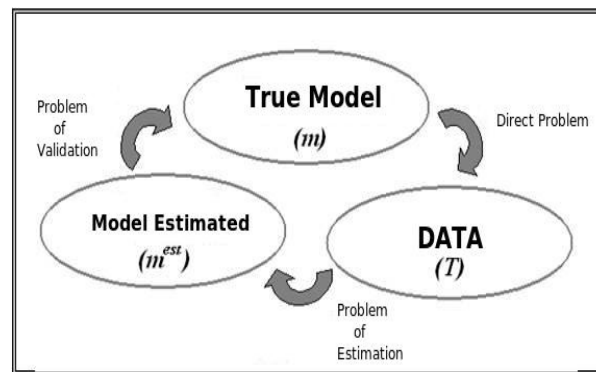
Figure 6: Canonic representation of optimization principle.

Controlled Random Search Global Method

The formalism applied was described by Price (1983) to solve the global optimization problem (Brachetti et al. (1997)), and a common characteristic to the global methods is that they attack two distinct problems at the same time:

1. The global search problem that is the exam of all region of interest aiming at to localize "more promising" sub-regions that contains the global minimum ($\mathbf{m}^{**}$);

2. The local search problem that is the determination of the global minimum ($\mathbf{m}^{**}$) using a local strategy, once a rather small neighborhood has been detected around the minimum.

As a simple description, it is desired with the Price method a solution of the global non-constrained optimization problem, structured in the following form: **min** $\phi(\mathbf{m})$, $\mathbf{m} \in R^M$, where $\phi : R^M \rightarrow R$ is a continuous function; that is, a minimum $\phi(\mathbf{m})$ of the continuous function is searched, where the parameter vector $\mathbf{m}$ (dimension M) to be determined is defined in the R^M space. In this form, $\mathbf{m}$ represents point-coordinates $m_i, (i = 1, M)$ in the continuous parameter space. The function object of minimizations is multi-modal.

To initiate the process, a V search domain is defined through the specification of explicit constraints to each parameter. Next, it is defined a predetermined quantity, N, of test points randomly chosen in V and consistent with the constraints (in case they are imposed) forming the set:

$$S_1^k = \left\{ \mathbf{m_1^{(k)}}, \mathbf{m_2^{(k)}}, \mathbf{m_3^{(k)}}, ..., \mathbf{m_N^{(k)}} \right\}. \tag{15}$$

The functional $\phi(\mathbf{m})$ is evaluated at each point N, and the position and value of the function $\phi(\mathbf{m})$ are saved in a matrix:

$$\mathbf{A}[Nx(N+1)]. \tag{16}$$

At each iteration a new test point P, $\widehat{\mathbf{m}}^{(k)}$, is calculated using a random sub-set $S_2^{(k)}$ of $S^{(k)}$ described in the form:

$$\widehat{\mathbf{m}}^{(k)} = \mathbf{c}^{(k)} - (\mathbf{m}_{20}^{(k)} - \mathbf{c}^{(k)}), \tag{17}$$

being $\mathbf{c}$ the centroid defined by:

$$c_j^{(k)} = \frac{1}{M} \sum_{i=1}^{M} m_{2i}^{(k)} \quad (j = 1, M). \tag{18}$$

Next, a test is made if the point P satisfies the constraints, and if

$$\phi(\widehat{\mathbf{m}}^{(k)}) < \phi(\widehat{\mathbf{m}}_{máx}^{(k)}). \tag{19}$$

In case these conditions are not satisfied, the process returns for new definitions. The probability that the points converge to the global minimum depends on the distribution, on the value of N, on the complexity of the functional, in the nature of constraints and in the choice of the test points. Figure 7 serves to exemplify the randomness of the misfit function $\phi(\mathbf{m})$ as a result of the automatic random selection of $\mathbf{m}$.
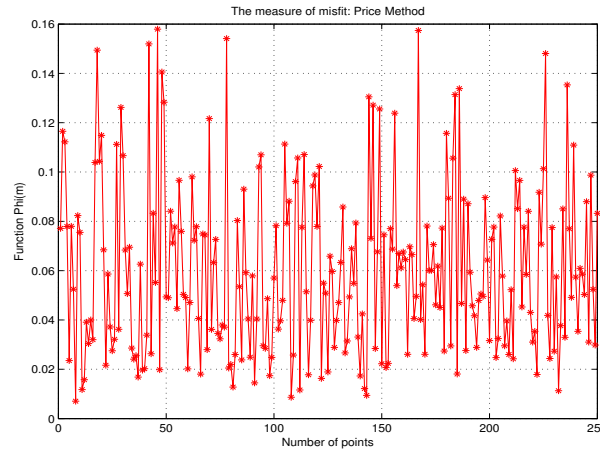
Figure 7: Price initial random non-fit function.

Gradient Method

This method is based on the multivariate Taylor series expansion of a function used to represent the observed data, that in this case is a seismic section. This series linearizes the problem to allow for an iterative solution based on the linear form $\mathbf{Gm} = \mathbf{t}$, where $\mathbf{G} \neq \mathbf{G}(\mathbf{m})$. The quantity $\mathbf{m}$ is the parameter vector to be resolved iteratively, and $\mathbf{G}$ the problem matrix. The data is represented by $\mathbf{t}(x_m, h; \mathbf{m_2})$, and the Taylor series expansion of the function $\mathbf{t}(x_m, h; \mathbf{m_2})$ in the neighborhood of $\mathbf{m_1}$ to the first order is mathematically written as:

$$t_i(x_m, h; \mathbf{m})|_{m=m_2} \approxeq t_i(x_m, h; \mathbf{m_1}) + \sum_{j=1}^{M} \frac{\partial t_i}{\partial m_j}(x_m, h; \mathbf{m})\Delta m_j|_{m=m_1}. \quad (i = 1, N). \tag{20}$$

From this expression, the observed time vector is defined representing the random variable,

$$t_i(x_m, h; \mathbf{m_2}) = t_i^{obs}(x_m, h; \mathbf{m_2} = true) = t_i^{obs}(x_m, h), \tag{21}$$

and the predictive time vector representing the theoretical model,

$$t_i(x_m, h; \mathbf{m_1}) = t_i^{pre}(x_m, h; \mathbf{m_1} = model) = t_i^{pre}(x_m, h; \mathbf{m}). \tag{22}$$

From these definitions, with $\mathbf{m_1} = \mathbf{m}$

$$t_i^{obs}(x_m, h) - t_i^{pre}(x_m, h; \mathbf{m}) = \sum_{j=1}^{M} \frac{\partial t_i^{pre}}{\partial m_j}(x_m, h; \mathbf{m})\Delta m_j, \tag{23}$$

that is conveniently rewritten in the matrix form,

$$\Delta \mathbf{t}(x_m, h; \mathbf{m}) = \mathbf{G}(x_m, h; \mathbf{m})\Delta \mathbf{m}. \tag{24}$$

This equation represents a linearized form to obtain a solution to the nonlinear problem. In this equation, $\Delta \mathbf{t}(x_m, h; \mathbf{m})$ is a column vector, $(Nx1)$, that represents the data deviations; $\Delta \mathbf{m}$ is a column vector, $(Mx1)$, that represents the parameter deviations; and $\mathbf{G}(x_m, h; \mathbf{m})$ is the problem matrix, (NxM), that has the data information along the columns, the parameter information along the lines, and is given by the partial derivatives in the form:

$$G_{i,j} = \frac{\partial t_i^{pre}}{\partial m_j}(x_{m_i}, h_i; \mathbf{m}), \quad (i = 1, N; j = 1, M) \tag{25}$$

These partial derivatives are rather long, and they are used to represent the sensibility functions with respect to the parameters. The continuous partial derivative with respect to v_0, and shown in Figure 9, is given by:

$$\frac{\partial t}{\partial v_0}(x_m, h) = \frac{-\frac{2t_0\left(\frac{h^2}{R_{NIP}} + \frac{(x_m-x_0)^2}{R_N}\right)\cos^2\alpha_0}{v_0^2} - \frac{4(x_m-x_0)^2\sin\alpha_0\left(t_0 + \frac{2(x_m-x_0)^2\sin\alpha_0}{v_0}\right)}{v_0^2}}{2\sqrt{\frac{2t_0\left(\frac{h^2}{R_{NIP}} + \frac{(x_m-x_0)^2}{R_N}\right)\cos^2\alpha_0}{v_0} + \left(t_0 + \frac{2(x_m-x_0)^2\sin\alpha}{v_0}\right)^2}} \tag{26}$$

The continuous partial derivative with respect to R_{NIP}, and shown in Figure 10, is given by:

$$\frac{\partial t}{\partial R_{NIP}}(x_m, h) = -\frac{h^2 t_0 \cos^2\alpha_0}{R_{NIP}^2 v_0 \sqrt{\frac{2t_0\left(\frac{h^2}{R_{NIP}} + \frac{(x_m-x_0)^2}{R_N}\right)\cos^2\alpha_0}{v_0} + \left(t_0 + \frac{2(x_m-x_0)^2\sin\alpha_0}{v_0}\right)^2}} \tag{27}$$

The continuous partial derivative with respect to R_N, and shown in Figure 11, is given by:

$$\frac{\partial t}{\partial R_N}(x_m, h) = -\frac{t_0(x_m-x_0)^2\cos^2\alpha_0}{R_N^2 v_0 \sqrt{\frac{2t_0\left(\frac{h^2}{R_{NIP}} + \frac{(x_m-x_0)^2}{R_N}\right)\cos^2\alpha_0}{v_0} + \left(t_0 + \frac{2(x_m-x_0)^2\sin\alpha_0}{v_0}\right)^2}} \tag{28}$$

The continuous partial derivative with respect to α_0, and shown in Figure 12, is given by:

$$\frac{\partial t}{\partial \alpha_0}(x_m, h) = \frac{\frac{4(x_m-x_0)^2\cos\alpha_0\left(t_0 + \frac{2(x_m-x_0)^2\sin\alpha_0}{v_0}\right)}{v_0} + \frac{2t_0\left(\frac{h^2}{R_{NIP}} + \frac{(x_m-x_0)^2}{R_N}\right)(\cos^2)'\alpha_0}{v_0}}{2\sqrt{\frac{2t_0\left(\frac{h^2}{R_{NIP}} + \frac{(x_m-x_0)^2}{R_N}\right)\cos^2\alpha_0}{v_0} + \left(t_0 + \frac{2(x_m-x_0)^2\sin\alpha_0}{v_0}\right)^2}} \tag{29}$$

From these partial derivatives, the quantities $\overline{S}_{ij} = \left.\frac{\partial\, ln\, t_i(\mathbf{m_0})}{\partial\, ln\, m_{0j}}\right|_{m_0} = \overline{S}_{ij}(\mathbf{m_0}) = \frac{m_{0j}}{t_{0i}}S_{ij}(\mathbf{m_0})$, are calculated, as in equation (6). From their plots, these functions present a general linear trend behavior in the $t-x$ window, which means that they do not show a specific form that could better define the resolution. In this case, the operator presents low resolution being necessary good starting point for the optimization, and even the possibility of a priori constraints.

In the least-square sense, the optimization problem is defined as over-determined (pure), the number of data greater then the number of parameters to be resolved for, $(N > M)$, and all parameters considered to have the same sampling. The minimization method starts with the principle that $\partial\phi(\mathbf{m})/\partial m_j = 0$, what establishes a local minimum. The linearization of the optimization problem is represented by equation $\mathbf{G}\Delta\mathbf{m} = \Delta\mathbf{t}$, where $\mathbf{G} = \mathbf{G}(\mathbf{m})$. The iterative solution of the nonlinear problem is represented by the equation:

$$\Delta\mathbf{m} = [\mathbf{G}^T\mathbf{G}]^{-1}\mathbf{G}^T\Delta\mathbf{t}. \tag{30}$$

The parameter update during the iterations is given by:

$$\mathbf{m}^{(k+1)} = \mathbf{m}^{(k)} + \gamma\Delta\mathbf{m} \tag{31}$$

where γ is an attenuation/amplification factor for the found solution $\Delta\mathbf{m}$, and k is the iteration number in the optimization process cycle.

Resolution

A statistical analysis for the method is made by the Data and Parameter Resolutions Matrices, and by the Unitary Covariance Matrix (Menke (2002)). These matrices are attributes of the method involving the derivative matrix, $\mathbf{G}$, and its generalized inverse $\mathbf{G}^{-g}$, that in the present case has the form $\mathbf{G}^{-g} = [\mathbf{G}^T\mathbf{G}]^{-1}\mathbf{G}^T$. The parameter resolution matrix is given by:

$$\mathbf{R}_p = \mathbf{G}^{-g}\mathbf{G}, \tag{32}$$

and the data resolution matrix is given by:

$$\mathbf{R}_d = \mathbf{G}\mathbf{G}^{-g}. \tag{33}$$

The unitary covariance matrix is given by:

$$cov_u(\mathbf{m}) = \sigma^{-2}\mathbf{G}^{-g}\left[cov\ \mathbf{t}\right]\mathbf{G}^{-gT} = \mathbf{G}^{-g}\mathbf{G}^{-gT}. \tag{34}$$

Flow Diagram

The flow diagram description of the computer program developed by Vieira and Leite (2009) and Santos et al. (2009) is resumed as follows:

01- Start

02- Input: (1) Control parameters; (2) Model parameters; (3) Initial model parameters; (4) Inversion parameters.

03- Start iterations: Controlled Random Search.

04- End iterations: Controlled Random Search.

05- Start iterations: Least-squares.

06- Calculation: Forward model.

07- Calculation: Curve fit and test for ending the iterations.

08- Calculation: Derivatives of the predictive operator.

09- Calculation: Matrices.

10- Calculation: Parameter update.

11- Calculation: Convergence test.

12- Returns to 05.

13- Calculation: Parameter Resolution Matrix.

14- Calculation: Data Resolution Matrix.

15- Calculation: Unit Covariance Unitary matrix.

16- Calculation: Quantity of Solution matrix.
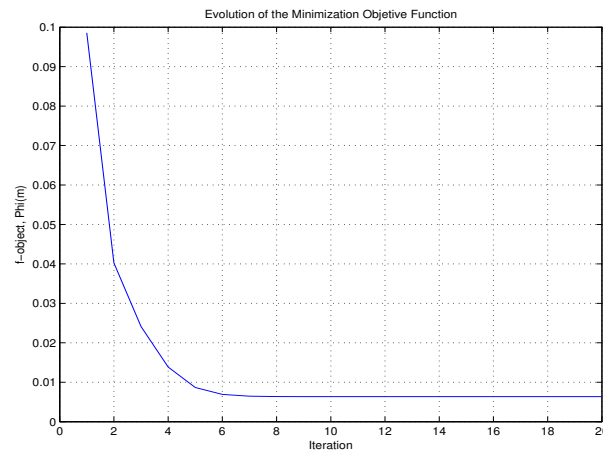
Figure 8: Evolution of the objective minimization function calculated in 20 iterations showing the stabilization of the process around the tenth iteration.

The CRSG method showed to be a strong allied in the strategy for the 4 parameters search of the forward model. The values obtained by the application of the CRSG and GM methods are presented in the table below, and it shows agreement between the results.

Parameters	Real	CRSG	GM
v_0 (m/s)	1500	1459,0	1445,8
R_{NIP} (m)	5000	5012,8	5112,3
R_N (m)	-5000	-4910,2	-4800,3
α_0 (radians)	0,2094	0,2019	0,2186

The following table represents the Normalized Parameter Resolution matrix(4X4) (32) that, should ideally have a unitary diagonal form, shows a weak scatter.

$\mathbf{R}_p$	v_0	R_{NIP}	R_N	α_0
v_0	1	0.287	-0.173	0.000
R_{NIP}	0.287	1	0.893	0.000
R_N	-0.173	0.893	1	0.000
α_0	0.000	0.000	0.000	1

The table below represents the Normalized Unitary Parameter Covariance matrix (4X4) (34), that should ideally have a diagonal unitary diagonal form, but shows a strong scatter, what corresponds to a non-desirable strong correlation between the parameters, and it says that by changing one parameter the others are also altered.

$cov_u(\mathbf{m})$	v_0	R_{NIP}	R_N	α_0
v_0	1	-0.832	-0.855	-0.362
R_{NIP}	-0.832	1	0.999	0.772
R_N	-0.855	0.999	1	0.750
α_0	-0.362	0.772	0.750	1.0

The maximum number of iterations allowed in the GM method was 20, and the evolution of the minimization object function is given by Figure 8. It was established that the solution strategy by the CRSG method was to be used as input to the GM method. But, the solutions in the above tables did not follow this strategy, and they were obtained in independent experiments for analysis.

CRS ATTRIBUTES SEARCH STRATEGY

In the practical applications of the CRS stack, the number of the attributes depends on the dimension of the problem (if 2-D or 3-D), and on the observation topography. For the flat observation surface, the applications considered only the search for the triplet R_{NIP}, R_N and α, with v_0 fixed, and to emphasize the present investigation, we follow the descriptions of Muller (1999) and Mann (2002), but not from the point of view of stack algorithm implementation. Their descriptions follows the criteria that the triplet search is a nonlinear optimization problem, that to be solved needs a starting point obtained in three major steps, with a last step as the final simultaneous triplet search. The searches are performed in the CMP bin, and the picking associated with the maximum coherency to simulate the corresponding ZO point.

- **First step**. This is one-parameter search for the combined v_{stack} performed to obtain a ZO section with $x_m = x_0$ in equation (1) that reduces it to:

$$t(x_m, h)|_{x_m=x_0} = \sqrt{t_0^2 + 2\frac{t_0}{v_0}\cos^2\alpha_0\frac{h^2}{R_{NIP}}}; \qquad (35)$$

  that, compared with $t(h) = \sqrt{t_0^2 + \dfrac{4h^2}{v_{NMO}^2}}$, the stacking velocity can be expressed in terms of α_0 and R_{NIP}, for $v_{NMO} = v_{stack}$, as

$$v_{stack}^2 = \frac{2v_0 R_{NIP}}{t_0 \cos^2\alpha_0}. \qquad (36)$$

  We call this step Automatic NMO stack (CMP stack), and it represents a non-iterative velocity analysis.

- **Second step**. This is one-parameter search for non-combined α_0 performed to obtain a ZO section with $h = 0$ and $R_N = \infty$ in equation (1) that reduces it to:

$$t(x_m, h)|_{(h=0, R_N=\infty)} = t_0 + \frac{2}{v_0}(x_m - x_0)\sin\alpha_0, \qquad (37)$$

  This first-order approximation can be regarded as a plane wave approximation, and this step is called Automatic Plane Wave stack, from where the emergence angle α_0 is obtained based on a small aperture. Inserting this angle into equation (36), a solution for R_{NIP} is found.

- **Third step**. This is one-parameter search for the non-combined R_N performed to obtain a ZO section with $h = 0$ in equation (1) that reduces it to:

$$t(x_m, h)|_{(h=0)} = \sqrt{\left[t_0 + \frac{2}{v_0}(x_m - x_0)\sin\alpha_0\right]^2 + \frac{2}{v_0}t_0\cos^2\alpha_0\frac{(x_m - x_0)^2}{R_N}}. \qquad (38)$$

  The values of α_0 and R_{NIP} would already be known from a previous step. This search is called Automatic Hyperbolic stack for R_N.

- **Fourth step**. This is one-parameter search for the non-combined R_{NIP} performed to obtain a ZO section with $R_N = \infty$ in equation (1) that reduces it to:

$$t(x_m, h)|_{(R_N=\infty)} = \sqrt{\left[t_0 + \frac{2}{v_0}(x_m - x_0)\sin\alpha_0\right]^2 + \frac{2}{v_0}t_0\cos^2\alpha_0\frac{(h)^2}{R_{NIP}}}. \qquad (39)$$

  The values of α_0 and R_N would already be known from a previous search step. This search is called Automatic Hyperbolic stack for R_{NIP}.

- **Fifth step**. In the practical applications (with v_0 fixed), with the parameters obtained from the previous steps, and in form of time sections, the traveltime surfaces can be calculated with equation (1). This subsequent stack can be performed to obtain a ZO stack that is called Initial CRS stack.

- **Sixth step**. In the practical applications (with v_0 fixed), with the parameters obtained in form of time sections as initial values, equation (1) is used for the simultaneous search which provides the Optimized CRS stack.

RESULTS

Several experiments were performed to analyze the behavior of the chosen sensibility function $\overline{S}_{ij} = \frac{\partial \, ln \, t_i(\mathbf{m}_0)}{\partial \, ln \, m_{0j}}\Big|_{m_0} = \overline{S}_{ij}(\mathbf{m}_0) = \frac{m_{0j}}{t_{0i}} S_{ij}(\mathbf{m}_0)$, as given by equation (6). The selected examples are presented in Figures 9, 10, 11 and 12, where the nominal values were: $v_0 = 1500 m/s$, $R_{NIP} = 5000m$, $R_N = -5000m$ and $\alpha_0 = +(\pi/15)rad$. The values chosen for $t_{0i}, (i = 1, 2, 3, 4, 5)$ were: $t_0 = (0.25, 0.50, 1.00, 2.00, 2.50, 3.00, 4.00, 5.00)$ in seconds.

The map for the derivative $(v_0/t_0)*\partial t(x_m, h; \mathbf{m})/\partial v_0$ of equation (26), plotted in Figure 9, is presented for four values of $t_{0i} = (0.5, 2.00, 4.0, 5.00s)$. The variation is still smooth, but faster than for the other three parameters. The maps indicate the nonlinear dependency with respect to the coordinates x_m and h. Therefore, has no ideal direction for its initial evaluation, and would be totally dependent on t_{0i}. Therefore, fixing the value of v_0 is consistent with this analysis over S_{ij}.

As can be seen in Figures 10, 11 and 12 only two values for $t_{0i} = (0.25, 5.00s)$ were necessary to show because the variation is very smooth.

The map for the derivative $(R_{NIP}/t_0) * \partial t(x_m, h; \mathbf{m})/\partial Rnip$ of equation (27), plotted in Figure 10, indicates the linear dependency with respect to the coordinates x_m, and constant with respect to h; therefore, this parameter would be better determined in sections where h =constant. In the attributes search strategies, a combination of the first and second steps would have to solve for R_N. Equation (39), with independent variable h, has the form of equation (38), with independent variable x_m. Figure 12 suggests consistency in the search for R_{NIP}, but not in accordance with Figure 10 and equation (39).

The map for the derivative $(R_N/t_0) * \partial t(x_m, h; \mathbf{m})/\partial Rn$ indicates also a strong linear dependency with respect to the coordinates h, and almost constant with respect to the coordinate x_m, therefore this parameter would be better determined in sections where x_m =constant.

The map for the derivative $(\alpha_0/t_0) * \partial t(x_m, h; \mathbf{m})/\partial \alpha_0$ indicates a strong linear dependency with respect to the coordinates h, and a weak linear dependence with respect to the x_m coordinate, therefore this parameter would be better determined in sections with x_m =constant.

In the **first step** for the CRS attributes search strategy, the combined one-parameter search for $v_{stack} = \sqrt{\frac{2v_0 R_{NIP}}{t_0 \cos^2 \alpha_0}}$ takes $x_m = x_0$ in equation (1) to have it in the form of equation (35), and has h as independent variable. This is consistent with the analysis with $\overline{S}_{ij}$ shown in Figure 12, and consistent with $\frac{\partial t(x_m, h)}{\partial h}\big|_{x_m=x_0}$ of equation (35).

In the **second step**, the non-combined one-parameter search for α_0 takes $h = 0$ and $R_N = \infty$ in equation (1) to have it in the form of equation (35), which is linear along the x_m coordinate, admits small values of x_m, and is consistent with Figure 12, and with $\frac{\partial t(x_m, h)}{\partial \alpha_0}\big|_{h=0, R_N=\infty}$ of equation (37).

In the **third step**, the search for the non-combined R_N takes $h = 0$ in equation (1) to have it in the form of equation (38), which is hyperbolic along the x_m coordinate. This result is consistent with Figures 12 and 11.

In the **fourth step**, the search for the combined parameter R_{NIP} takes $R_N = \infty$ in equation (1) to have it in the form of equation (39), which is hyperbolic along the h coordinate.
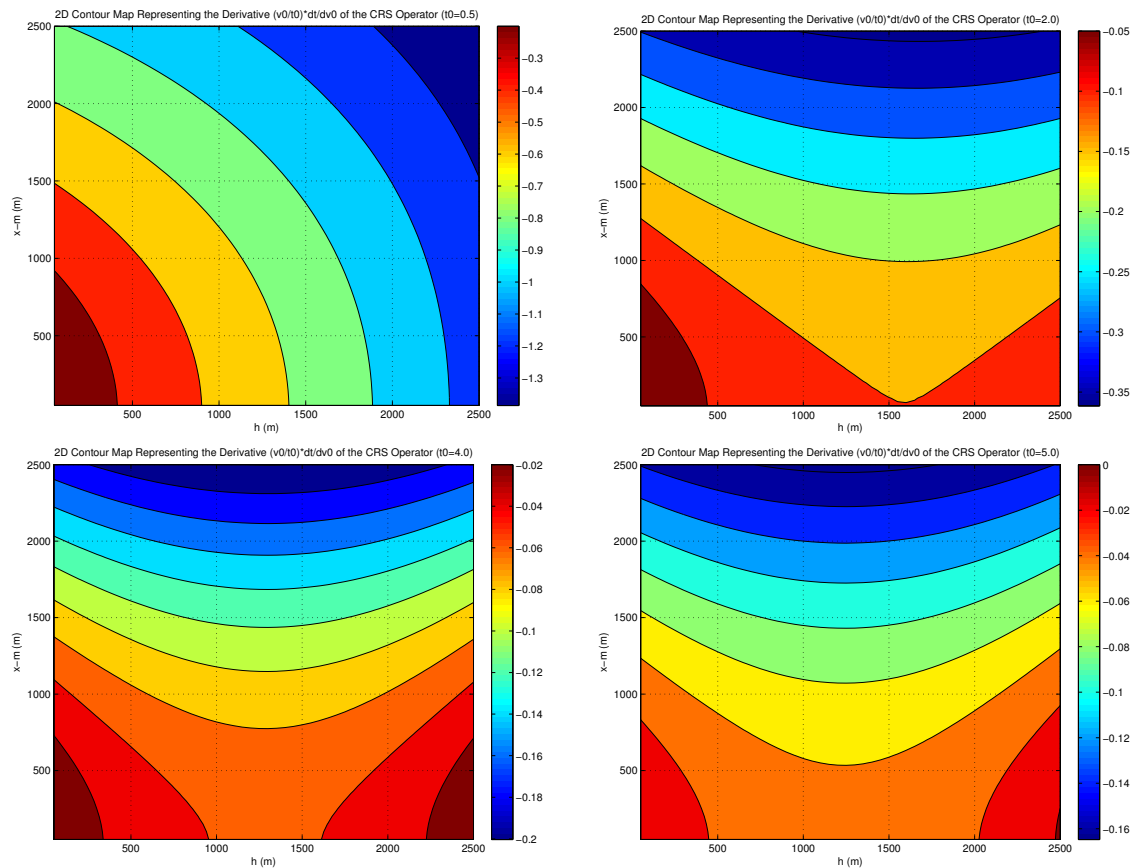
Figure 9: Contour maps of the normalized derivative $(v_0/t_0) * \partial t(x_m, h; \mathbf{m})/\partial v_0$ of the forward model indicating the linear dependency with respect to the coordinates x_m and h. Consequently, the parameter v_0 has no special sections for its determination. (Top left: $t_0 = 0.50s$), (Top right: $t_0 = 2.00s$), (Bottom left: $t_0 = 4.00s$), (Bottom right: $t_0 = 5.00s$).
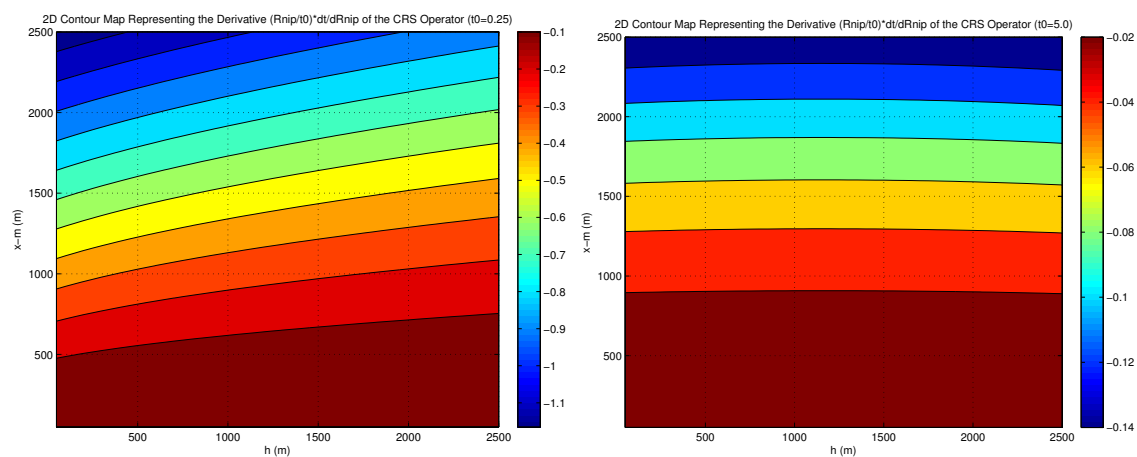
Figure 10: Contour maps of the normalized derivative $(R_{NIP}/t_0) * \partial t(x_m, h; \mathbf{m})/\partial Rnip$ of the forward model indicating the linear dependency with respect to the coordinates x_m, and constant with respect to h. Consequently, the parameter R_{NIP} is better determined in sections of h =constant (CO). (Left: $t_0 = 0.25s$), (Right: $t_0 = 5.00s$).
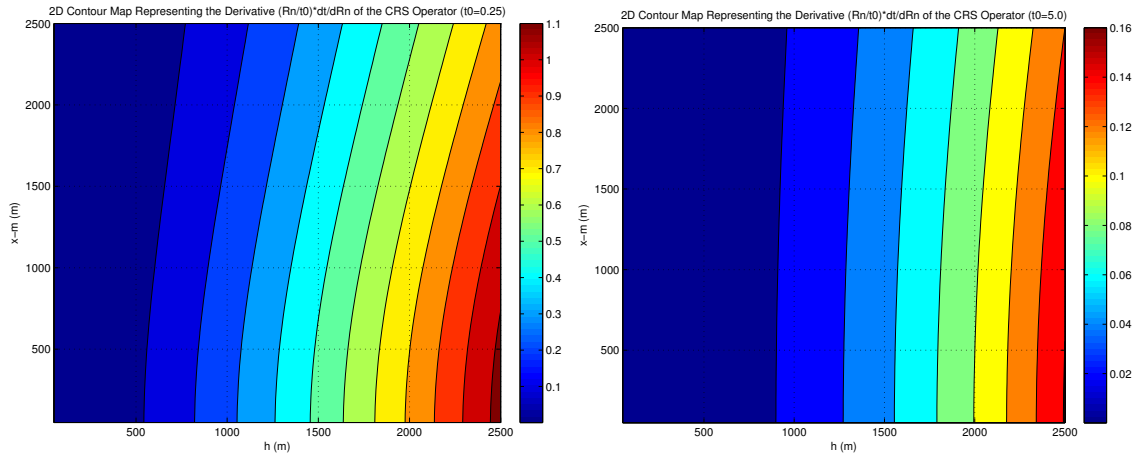
Figure 11: Contour maps of the normalized derivative $(R_N/t_0) * \partial t(x_m, h; \mathbf{m})/\partial Rn$ of the forward model indicating a strong linear dependency with respect to the coordinates h, and almost constant with respect to the coordinate x_m. Consequently, the parameter R_N is better determined in sections of $x_m =$constant (CMP). (Left: $t_0 = 0.25s$), (Right: $t_0 = 5.00s$).
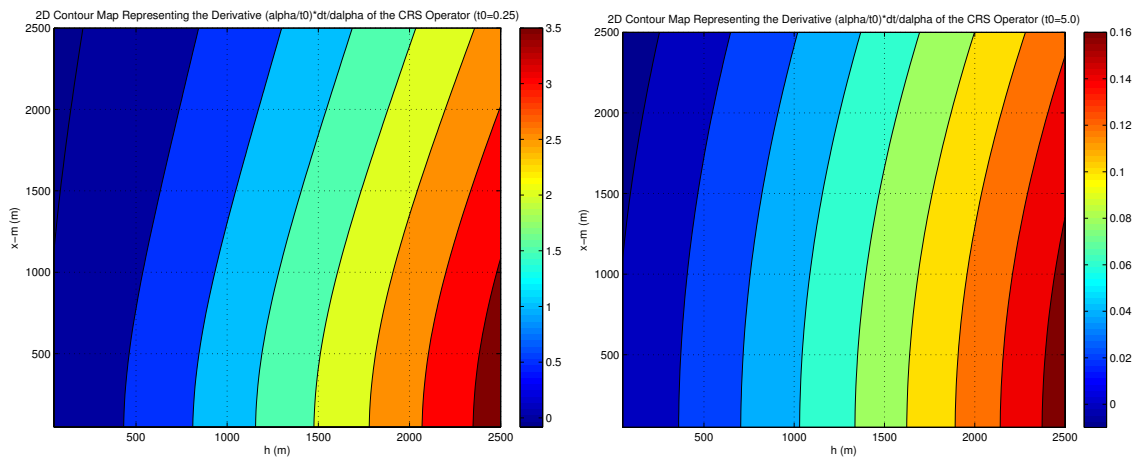
Figure 12: Contour maps of the normalized derivative $(\alpha_0/t_0) * \partial t(x_m, h; \mathbf{m})/\partial \alpha_0$ of the forward model indicating a strong linear dependency with respect to the coordinates h, and a weak linear dependence with respect to the x_m coordinate. Consequently, the parameter α_0 is better determined in sections of $x_m =$constant (CMP). (Left: $t_0 = 0.25s$), (Right: $t_0 = 5.00s$).

CONCLUSIONS

We investigate the relationship between sensitivity analysis, $\mathbf{S}$, of the CRS operator with respect to the parameters v_0, R_{NIP}, R_N and α_0, and comparing with the attributes search strategies that is based on physical-mathematical considerations of the stack operator.

In the CRS stack method, the velocity v_0 is admitted as fixed, but it has a physical representation as shown by the model of Figure 2, and, in practical terms, it represents an average taken along the observation geophone spread window, and represents a sampling over the upper layers under the dominant wavelength of the source-effective pulse. This strategy is fully consistent with the $\mathbf{S}$ analysis.

Even though there is a strong linear behavior of the derivatives in the spatial window (x_m, h), a different strategy for the parameter search was not here provided.

For the parameter resolution, it would be desirable a concave form of the object function of opti-

mization. Even though, we concluded that the CRS operator under such measures present low resolution capacity. of resolution. In this way, it is necessary a good start point for the optimization that searches for the three parameters (v_0 =fixed, R_{NIP}, R_N e α_0) simultaneously. From the point of view of the sensitivity function, it would be necessary to employ constraints as a priori conditions for the simultaneous parameter optimization.

The tests were performed for a fixed point $P_0(x_0, t_0)$, and a next step would be for points randomly chosen along a trace, ($t_0 = 0, t_{total}$), and next for a any point along the CMP.

Once established a form to represent the resolution and sensibility of the $t(x_m, h; v_0, R_{NIP}, R_N, \alpha_0)$ function to its parameters, a next step would be to repeat the experiment based on a form of modified semblance.

ACKNOWLEDGMENTS

REFERENCES

Bernabini, M., Carrion, P., Jacovitti, G., Rocca, F., Treitel, S., and Worthington, M., editors (1987). *Deconvolution and Inversion*. Blackwell Scientific Publications.

Brachetti, P., Ciccoli, M. D. F., Pillo, G. D., and Lucidi, S. (1997). A new version of price's algorithm for global optimization. *Journal of Global Optimization*, pages 165–184.

Frank, P. M. (1978). *Intoduction to System Sensitivity Theory*. Academic Press.

Mann, J. (2002). *Extensions and applications of the common-reflection-surface stack method*. Universitat Karlsruhe, Germany.

Menke, W. (2002). *Geophysical Data Analysis: Discrete Inverse Theory*. Academic Press.

Muller, T. (1999). *The Common Reflection Surface Stack - Seismic Imaging Without Explicit Knowledge of the Velocity Model*. Universitat Karlsruhe, Germany.

Price, W. (1983). Global optimizationby controlled random search. *Journal of Optimization Theory and Applications*, 40(3):333–348.

Saltelli, A., Tarantola, S., Campolongo, F., and Ratto, M. (2004). *Sensitivity Analysis in Practice. A Guide to Assessing Scientific Models*. John Wiley and Sons.

Santos, R., Leite, L., and Vieira, W. (2009). Otimização do operador de empilhamento crs. *11th International Congress of the Brazilian Geophysical Society. Salvador, Bahia, Brazil.*

Tarantola, A. (1984). *Inverse Problem Theory*. SIAM.

Vieira, W. and Leite, L. (2009). Sensibilidade e resolução dos parâmetros do operador de empilhamento crs. *Workshop da Rede Cooperativa de Geofísica de Exploração. Salvador, Bahia, Brazil.*